Chinese Journal of Electronics
vol. 33, no. 3, pp. 823–832, May 2024
https://doi.org/10.23919/cje.2022.00.159

RESEARCH ARTICLE

Joint Optimization of Trajectory and Task Offloading for Cellular-Connected Multi-UAV Mobile Edge Computing

Jingming XIA[1], Yufeng LIU[2], and Ling TAN[2]

1. *School of Artificial Intelligence, Nanjing University of Information Science and Technology, Nanjing 210044, China*
2. *Engineering Research Center of Digital Forensics Ministry of Education, Nanjing University of Information Science and Technology, Nanjing 210044, China*

Corresponding author: Ling TAN, Email: cillatan0@nuist.edu.cn
Manuscript Received June 2, 2022; Accepted December 9, 2022

Abstract — Since the computing capacity and battery energy of unmanned aerial vehicle (UAV) are constrained, UAV as aerial user is hard to handle the high computational complexity and time-sensitive applications. This paper investigates a cellular-connected multi-UAV network supported by mobile edge computing. Multiple UAVs carrying tasks fly from a given initial position to a termination position within a specified time. To handle the large number of tasks carried by UAVs, we propose a energy cost of all UAVs based problem to determine how many tasks should be offloaded to high-altitude balloons (HABs) for computing, where UAV-HAB association, the trajectory of UAV, and calculation task splitting are jointly optimized. However, the formulated problem has nonconvex structure. Hence, an efficient iterative algorithm by applying successive convex approximation and the block coordinate descent methods is put forward. Specifically, in each iteration, the UAV-HAB association, calculation task splitting, and UAV trajectory are alternately optimized. Especially, for the nonconvex UAV trajectory optimization problem, an approximate convex optimization problem is settled. The numerical results indicate that the scheme of this paper proposed is guaranteed to converge and also significantly reduces the entire power consumption of all UAVs compared to the benchmark schemes.
Keywords — Unmanned aerial vehicles, High-altitude balloons, Mobile edge computing, Task splitting, Block coordinate descent.
Citation — Jingming XIA, Yufeng LIU, and Ling TAN, “Joint Optimization of Trajectory and Task Offloading for Cellular-Connected Multi-UAV Mobile Edge Computing,” *Chinese Journal of Electronics*, vol. 33, no. 3, pp. 823–832, 2024. doi: 10.23919/cje.2022.00.159.

I. Introduction

Currently, Unmanned aerial vehicles (UAVs) have received extensive focus from academia and industry ascribed to the little size, cost-effectiveness and strong mobility [1]–[5]. Hence, UAVs appear in a variety of well-received applications, among which the advantages of UAVs as aerial mobile users [6] should not be underestimated. Nonetheless, in the 6G network, some related applications of cellular-connected UAVs are emerging one after another [7], potentially introducing unparalleled challenges to the computational capabilities of UAVs owing to their restricted calculation capacity. Fortunately, mobile edge computing (MEC) is envisioned as a ground-breaking approach to perform computation at the edge of the networks [8]–[11]. Specifically, the UAV carrying high computational complexity or time-sensitive missions is able to cooperate with the ground base stations (GBSs), which own MEC servers [12]–[14], which allows that the cellular-connected network provides UAVs with computing service supports. By these particular features, MEC can potentially improve the computing performance of UAV efficiently [15].

In practice, the GBSs may be largely damaged after natural disasters or the ground is not suitable for building GBSs due to geographical defects. In this case, how to quickly complete the computational tasks of the UAVs for carrying computation-intensive and delay-sensitive

Associate Editor: Prof. Chenren XU, Peking University.

tasks is an important issue. In [16], the authors developed the architecture of a two-layer UAV in the MEC network, where the low-altitude platform UAVs (LAP-UAVs) offload the computing tasks to the high-altitude platform UAVs (HAP-UAVs) equipped with MEC servers. However, the LAP-UAVs carrying the computing tasks are positioned in advance and the mobility of LAP-UAVs is not involved. In addition, when the number of missions carried by LAP-UAVs increases, the resources of HAP-UAVs is often limited.

Recently, high-altitude balloons (HABs) are attracting much attention because of their low deployment cost and wide coverage [17], which have been applied in many fields, involving communication, liaison, and investigation [18]. In particular, when the wireless transmissions between the ground users and the GBSs are inconvenient, HABs can act as a communication relay between the ground users and the GBSs [19] such that the tasks carried by users on the ground can be better completed. However, the long-distance transmission may lead to significant delays, which is very unfriendly for some delay-sensitive tasks. Therefore, in order to reduce task transfer latency and enable HABs to process computing locally, MEC can be deployed locally on each HAB [20]. In this sense, when MEC-supported HABs receive tasks from ground users, they can use their strong computing power to process the offloaded tasks by themselves, without the need to further transmit them to remote GBSs or cloud, which is of great significance for time-sensitive tasks. Furthermore, HABs are capable of quickly arranging in the stratosphere and the energy consumption caused by hovering can be reduced to some extent [21]. As the aerial flying users, UAVs have also stronger and more reliable visual range links with HABs, which allows each UAV to connect to multiple HABs simultaneously, leveraging their distributed computing resources to increase computing power. And it's a huge breakthrough for dealing with situations where the GBSs are not built on the ground or they are damaged. Accordingly, it is an interesting research topic to plan the UAVs' trajectory and to select which HABs to unload computational tasks in the whole flight process aiming to minimize the energy cost.

Sparked by the above discussions, this paper considers a multi-HAB-enabled MEC network, where multiple UAVs depart from a given initial position and fly to a given termination position. During the flight of UAVs, they need to complete their computing tasks. We suppose that the UAVs can divide tasks into smaller subtasks, and simultaneously they can unload tasks to several HABs selected for the parallel process. In this setting, the intent is to make the energy that all UAVs consumed minimization through joint optimization of UAV-HAB association, the trajectory of UAV, and calculation mission splitting.

For clarity, the significant contributions of this paper are as follows:

- We propose a two-layer computing system considering both multi-UAV and multi-HAB, where a task partitioning strategy is furnished to oversee the allocation of computing tasks. We investigate the joint optimization problem of UAV-HAB association, UAV trajectory, and computation task splitting in terms of energy consumption, while considering the constraints related to delay and speed.
- Considering the complexity and nonlinearity of the formulated optimization problem, the binary variables for UAV-HAB association are first relaxed into continuous variables and an iterative optimization algorithm based on descent (BCD) is proposed to realize near-optimal solution with remarkably reduced complexity. In particular, all optimization variables are divided into two blocks for UAV-HAB association, calculation task splitting and UAV trajectory, respectively. Afterwards, at each iteration, the two blocks of variables are alternately optimized. Nevertheless, even with fixed UAV-HAB association and calculation task splitting, the UAV trajectory optimization problem with the nonconvex structure is still difficult to solve. Therefore, the successive convex approximation (SCA) method is applied to settle this issue.
- In order to prove the feasibility and effectiveness of the solution proposed in this paper, we provide a comprehensive verification work, and the results demonstrate that the proposed method can achieve near-optimal performance in reducing the energy consumption, compared with other schemes. The impacts of different parameters are also analyzed.

The rest of this paper is arranged as follows. Section II provides a discussion on the relevant literature. Section III is dedicated to elucidating the system model and formulating the optimization problem. In Section IV, we demonstrate a solution to the considered problem with SCA technique and propose a BCD-based iterative algorithm. The computational complexity and the convergence of the proposed algorithm is analyzed in Section V. Section VI provides detailed numerical results, while Section VII presents the conclusions.

II. Related Work

The mainstream studies on UAV-enabled MEC is briefly elaborated as follows.

UAV-enabled MEC supplies extensive coverage for computing offloading compared to terrestrial MEC networks. The work in [22] considered a UAV-enabled MEC to supply caculation support to Internet of things (IoT) devices with strict deadlines and maximized the number of IoT devices served. The authors in [23] investigated a cooperative UAV-enabled MEC network structure in which UAVs can aid other UAVs to carry out caculating missions. A UAV-enabled MEC platform was investigated in [24], where the average UAV energy consumption and data queue stability were taken into account. However, the above existing works only state that UAV plays the role of aerial base station.

Due to the growing concern over UAV as aerial mobile user, there exists some works related with the UAV-based computing service. For instance, in [25], the authors were aimed at minimizing the mission completion time of UAV by optimizing the flight trajectory of the UAV and calculation offloading scheduling. In [26], based on the comprehensive consideration of energy and time constraints, the authors chose the best cooperative object between the GBSs and the neighboring UAV to carry out the offloading of the computing tasks. For the UAVs with insufficient endurance, it is of great significance in many applications to optimize their energy consumption and then prolong the flight time. In this regard, the authors of [27] and [28] comprehensively considered the UAV trajectory, calculation task allocation, and transmission power with the purpose of minimizing the overall energy consumption in a cellular-connected UAV MEC network. For the cellular-connected multi-UAV MEC scenario, the work in [29] focused on optimizing the total energy consumption of the UAVs by taking the energy restriction and resource constraint of the terrestrial base stations (TBSs) into account. These excellent efforts are devoted to the computational task offloading between single UAV/multi-UAV and single GBS/multi-GBS in the context of MEC.

Different from the aforementioned studies, we investigate the problem of multi-HAB-enabled MEC network in this paper to assist multiple UAVs to complete computing tasks and minimize their energy consumption simultaneously.

III. System Model and Problem Formulation

A multi-UAV network supported by MEC is depicted in Figure 1. In this network, there are some UAVs with cellular connections, each of them has a specific number k, where $k \geq 1$ and $k \in \mathcal{K} \triangleq \{1, 2, \ldots, K\}$, while a set $\mathcal{M} \triangleq \{1, 2, \ldots, M\}$ of $M \geq 1$ HABs with MEC servers. During a given period T, multiple UAVs fly from the initial location to the final location respectively, and meanwhile need to complete the calculation tasks carried by themselves. The partial computation offloading mode is studied where the task can be executed by the UAV and the served HABs collaboratively. It is assumed that the task quantity carried by UAV k is L_k ($L_k > 0$), the UAV k computes part of the tasks by itself, with the ratio ρ_k, and uninstalls the remaining tasks with the ratio of $(1 - \rho_k)$ to the MEC servers on HABs to provide remote computing assistance. Obviously, $0 \leq \rho_k \leq 1$, $\rho_k = 0$ means that UAV k uninstalls all tasks to HABs, $\rho_k = 1$ means that UAV k calculates the entire tasks locally. Because the size of the calculation results is always much smaller than that of the task input, we assume that the time for HABs to return the calculation results to the UAVs is negligible [25].

For a three dimensional Cartesian coordinate system, all UAVs fly at a fixed altitude H_1 ($H_1 > 0$) and their horizontal position at the time instant $t \in [0, T]$ is expressed as $\boldsymbol{u}_k = [x_k(t), y_k(t)]^{\mathrm{T}}$, $k \in \mathcal{K}$. To make the problem considered easier to deal with, we equally divided the time T of the task completion into N parts, and the size of each time slot is δ_t. Hence, the horizontal position of UAV k is expressed as $\boldsymbol{u}_k[n] = \boldsymbol{u}_k(n\delta_t), n \in \mathcal{N} \triangleq \{1, 2, \ldots, N\}$. Besides, within each time slot, the speed of the UAV remains the same, where the speed of UAV k is expressed as $\boldsymbol{v}_k[n]$, $k \in \mathcal{K}$, $n \in \mathcal{N}$. In addition, compared with existing work, the advantages of the proposed multi-UAV network are as follows, on one hand, it can make up for the lack of calculation ability of the UAV. On the other hand, it can cope well with the situation that the ground base station does not exist or is damaged.

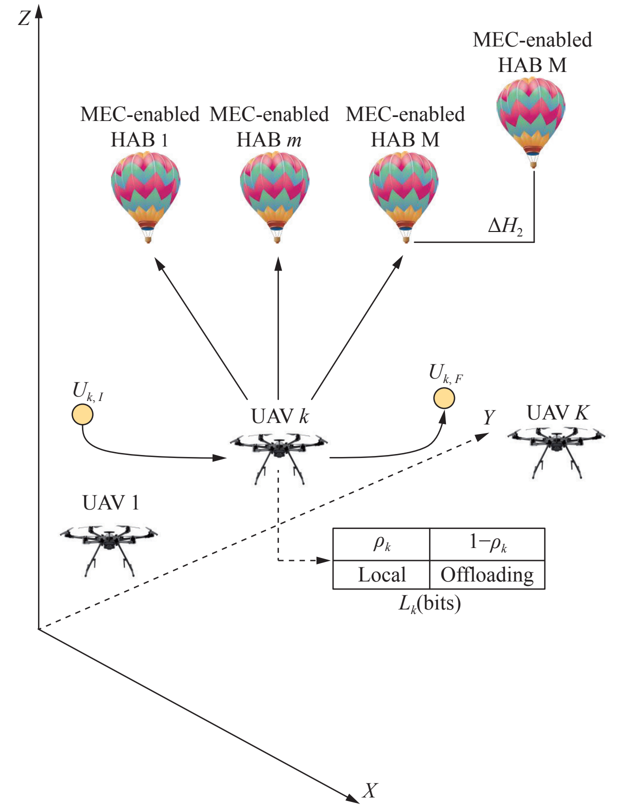

Figure 1 A two-layer computing architecture consisting of multi-UAV and multi-HAB, where the tasks of multi-UAV are offloaded to HABs during flight.

1. Channel model

Assume that the initial hover height of each HAB $m \in \mathcal{M}$ is H_2 ($H_2 > H_1$), and affected by factors such as wind and air pressureand, the range of fluctuation and drift is ΔH_2. Thus, the altitude of HAB m is $(H_2 + \Delta H_2)$, where $\Delta H_2 \in [-1, 1]$. Meanwhile, HAB m is fixed at the horizontal position $\boldsymbol{w}_m = [x_m, y_m]^{\mathrm{T}}, m \in \mathcal{M}$. Therefore, the distance from UAV k to HAB m is expressed as

$$d_k(m) = \sqrt{\|\boldsymbol{u}_k[n] - \boldsymbol{w}_m\|^2 + (H_2 - H_1)^2} \tag{1}$$

Similar to [30]–[32], the line-of-sight (LoS) link and free-space path-loss model are considered. As such, the channel power gain from UAV k to HAB m can be expressed as

$$h_{k,m}[n] = \frac{\beta_0}{d_{k,m}^2[n]} = \frac{\beta_0}{\|\boldsymbol{u}_k[n] - \boldsymbol{w}_m\|^2 + (H_2 - H_1)^2} \quad (2)$$

where β_0 stands for the channel power gain.

In this system, the time-division-multiple-access (TDMA) technology is exploited to limit the computational offloading process of UAV [33], i.e., the UAV communicates with at most one HAB. Let $a_{k,m}[n]$ be a binary variable of UAV association that indicates whether UAV k is served by HAB m. If $\alpha_{k,m}[n] = 1$, HAB m receives the computation task from UAV k, otherwise $\alpha_{k,m}[n] = 0$. Thus, $\alpha_{k,m}$ needs to satisfy the following two constraints:

$$\alpha_{k,m}[n] \in \{0, 1\} \quad (3)$$

$$\sum_{m=1}^{M} \alpha_{k,m}[n] \le 1 \quad (4)$$

On the other hand, the trajectory $\boldsymbol{u}_k[n]$ of UAV k is constrained by velocity $\boldsymbol{v}_k[n]$, and the collision avoidance in each time slot n. These yield the constraints as follows:

$$\|\boldsymbol{v}_k[n]\| \le \boldsymbol{v}_{\max} \quad (5)$$

$$\boldsymbol{u}_k[0] = \boldsymbol{u}_{k,\mathrm{I}}, \quad \boldsymbol{u}_k[N] = \boldsymbol{u}_{k,\mathrm{F}} \quad (6)$$

$$\boldsymbol{u}_k[n+1] = \boldsymbol{u}_k[n] + \boldsymbol{v}_k[n]\delta_t \quad (7)$$

$$\|\boldsymbol{u}_k[n] - \boldsymbol{u}_j[n]\|^2 \ge d_{\min}^2 \quad (8)$$

Formula (5) indicates the limit of UAV's flight speed; formula (6) represents the setting of initial and terminal positions of UAV; formula (7) indicates the relationship between UAV position and speed; and formula (8) represents that there is a minimum distance between different UAVs to avoid the collision.

The transmit power of UAV k for offloading is defined as $p_k[n]$. Herein, the power of each UAV is assumed known. Then, the transmission rate of UAV k to HAB m is calculated as

$$R_{k,m}[n] = \alpha_{k,m}[n] B \log_2\left(1 + \frac{p_k[n] h_{k,m}[n]}{\sigma^2}\right) \quad (9)$$

where B is the bandwidth of the system and σ^2 signifies the additive white Gaussian noise power [34].

2. Energy consumption model

The energy consumption of UAV k contains local-calculation energy cost, communication energy cost, and flight energy cost. The details of each part of energy consumption are described as follows.

1) Local-calculation energy consumption

According to the relevant settings above, we can know that the task quantity that needs to be calculated at UAV k is $\rho_k L_k$, and the unit is set as bits. Consequently, the energy consumption of local calculation is given by

$$E_k^{\mathrm{loc}} = C_{\mathrm{u},k} P_{\mathrm{u},k} \rho_k L_k \quad (10)$$

where $C_{\mathrm{u},k}$ indicates the number of central processing unit (CPU) cycles required to compute a 1-bit size mission, and $P_{\mathrm{u},k}$ signifies the energy consumption of one CPU cycle. Besides, denoting $D_{\mathrm{u},k}$ as the frequency of CPU. Thus, the time consumed by the local calculation can be expressed as $C_{\mathrm{u},k} \rho_k L_k \left(D_{\mathrm{u},k}\right)^{-1}$.

2) Communication energy consumption

If UAV k offloads the mission to HAB m, the communication energy for offloading of UAV k is expressed as

$$E_k^{\mathrm{comm}} = \sum_{n=1}^{N} \alpha_{k,m}[n] p_k[n] \delta_t \quad (11)$$

3) Flight energy consumption

The power consumption associated with the flight of rotary-wing UAV k is expressed as [35]

$$\begin{aligned} P[\boldsymbol{v}_k[n]] =& P_0\left(1 + \frac{3\|\boldsymbol{v}_k[n]\|^2}{U_{\mathrm{tip}}^2}\right) + \frac{P_i V_0}{\|\boldsymbol{v}_k[n]\|} \\ &+ \frac{1}{2} d_0 \epsilon s M \|\boldsymbol{v}_k[n]\|^3 \end{aligned} \quad (12)$$

where P_0 and P_i represent the profile power and induced power of UAV in hovering state, U_{tip} stands for the blade tip speed of the rotor, V_0 represents the average induced rotor speed during forwarding flight, d_0 is the fuselage resistance ratio, s is the rotor compaction, ϵ represents the air density, and M denotes rotor disc area. Thus, during the flight time T, the energy consumed by UAV flight is calculated as

$$E_k^{\mathrm{fly}} = \sum_{n=1}^{N} P[\boldsymbol{v}_k[n]] \delta_t \quad (13)$$

3. Problem formulation

In this paper, we concentrate on the problem of joint UAV-HAB association, UAV trajectory, and calculation task splitting design with the objective of minimizing the total energy cost incurred by all UAVs. For the convenience of usage, the UAV-HAB association variable set can be modeled as $\boldsymbol{A} = \{\alpha_{k,m}[n], \forall k \in \mathcal{K}, \forall m \in \mathcal{M}, \forall n \in \mathcal{N}\}$, the variable set of UAV trajectory is modeled as $\boldsymbol{U} = \{\boldsymbol{u}_k[n], \boldsymbol{v}_k[n], \forall k \in \mathcal{K}, \forall n \in \mathcal{N}\}$, and the calculation task splitting ratio variable set can be modeled as $\boldsymbol{\varrho} = \{\rho_k, \forall k \in \mathcal{K}\}$. Under this circumstance, we formulate the corresponding problem as follows:

$$\text{P1:} \quad \min_{\boldsymbol{A},\boldsymbol{U},\boldsymbol{\varrho}} \sum_{k=1}^{K} E_k^{\text{loc}} + \sum_{k=1}^{K} E_k^{\text{comm}} + \sum_{k=1}^{K} E_k^{\text{fly}} \tag{14a}$$

$$\text{s.t.} \quad 0 \le \rho_k \le 1, \tag{14b}$$

$$\frac{C_{\mathrm{u},k}\rho_k L_k}{D_{\mathrm{u},k}} \le T, \tag{14c}$$

$$\sum_{n=1}^{N}\sum_{m=1}^{M}\left(\alpha_{k,m}[n] B \log_2\left(1+\frac{p_k[n]h_{k,m}[n]}{\sigma^2}\right)\right)\delta_t \ge (1-\rho_k)L_k, \tag{14d}$$

$$\text{Eqs. (3), (4), (5), (6), (7), (8).} \tag{14e}$$

where constraint (14b) represents the feasible and boundary constraints of the calculation task splitting ratio; constraint (14c) states that the task execution time calculated at the UAV terminal should not exceed the delay tolerance; constraint (14d) signifies the conditions satisfied by the total number of bits used for uplink transmission within a given task completion time T. In the constraint (14e), formulas (3) and (4) represent the association limits between the UAV and HAB; formula (5) represents the maximum speed limit of UAV; formula (6) denotes the initial position and terminational location of the UAV; formula (7) is the relationship between the horizontal position and velocity of UAV in two continuous time slots; and formula (8) indicates that there is a minimum distance between different UAVs to avoid the collision.

It can be readily observed that the UAV-HAB association constraints (3) and (4) involve integer variables $\boldsymbol{A}$. The objective function, the constraints (8) and (14d) are all nonconvex due to the highly coupled optimization variables with respect to $\boldsymbol{U}$ and $\boldsymbol{\varrho}$. As a result, the optimization problem (P1) is a nonconvex mixed integer non-linear programming problem, which cannot be solved by conventional convex optimization techniques.

In the following section, the original problem (P1) is divided into two more tractable subproblems, and an efficient alternative algorithm is proposed to attain a suboptimal solution that converges to the original problem.

IV. Proposed Solution

This section discusses the specific method for solving problem (P1).

To elaborate, we first deal with the binary UAV-HAB association variables where the processing method is similar to that mentioned in [13]. On this basis, the binary variables in $\boldsymbol{A}$ is relaxed into continuous variables and the primal problem (P1) is reconstructed as

$$\text{P2:} \quad \min_{\boldsymbol{A},\boldsymbol{U},\boldsymbol{\varrho}} \sum_{k=1}^{K} E_k^{\text{loc}} + \sum_{k=1}^{K} E_k^{\text{comm}} + \sum_{k=1}^{K} E_k^{\text{fly}} \tag{15a}$$

$$\text{s.t.} \quad 0 \le a_{k,m}[n] \le 1, \tag{15b}$$

$$\text{Eqs. (4), (5), (6), (7), (8), (14b), (14c), (14d).} \tag{15c}$$

Neverthless, the problem (P2) is remain a nonconvexity structure. Even so, (P2) can be efficiently settled by using the BCD method. More concretely, we divide the optimization variables of (P2) into two parts, i.e. $\{\boldsymbol{A}, \boldsymbol{\varrho}\}$ and $\boldsymbol{U}$. In this way, the complexity of the optimization problem is reduced to some extent. Hence, we then optimize the following two sub-problems iteratively to solve (P2). We first optimize the $\{\boldsymbol{A}, \boldsymbol{\varrho}\}$ under a given feasible $\boldsymbol{U}$, then we optimize $\boldsymbol{U}$ based on the optimized $\{\boldsymbol{A}, \boldsymbol{\varrho}\}$, the iterative approach based on the BCD method is employed to alternately solve the above two subproblems.

1. UAV-HAB association optimization

When the trajectory of UAVs $\{\boldsymbol{A}, \boldsymbol{\varrho}\}$ are given, problem (P2) is described as

$$\text{P2.1:} \quad \min_{\boldsymbol{A},\boldsymbol{\varrho}} \sum_{k=1}^{K} E_k^{\text{loc}} + \sum_{k=1}^{K} E_k^{\text{comm}} + \sum_{k=1}^{K} E_k^{\text{fly}} \tag{16a}$$

$$\text{s.t.} \quad \text{Eqs. (4), (14b), (14c), (14d), (15b)} \tag{16b}$$

Based on the problem of (P2.1), it is a standard linear program (LP) problem when the trajectory of UAV $\boldsymbol{U}$ is known, so we can effectively solve the problem by utilizing the optimization tool CVX.

2. UAV trajectory optimization

When the UAV-HAB association and calculation task splitting ratio $\{\boldsymbol{A}, \boldsymbol{\varrho}\}$ are given, we can get the problem as follows

$$\text{P2.2:} \quad \min_{\boldsymbol{U}} \sum_{k=1}^{K} E_k^{\text{loc}} + \sum_{k=1}^{K} E_k^{\text{comm}} + \sum_{k=1}^{K} E_k^{\text{fly}} \tag{17a}$$

$$\text{s.t.} \quad \text{Eqs. (5), (6), (7), (8), (14d)} \tag{17b}$$

It is clear that the constraints (5), (6) and (7) are all convex except the objective function, constraints (8) and (14d), which manifests that we cannot directly apply standard convex method. To address this, the relaxation variable $\{\lambda_{k,n}\}$ is introduced, then UAV k's flight energy consumption is denoted as $\overline{E}_k^{\text{fly}}$ and it can be represented as

$$\overline{E}_k^{\text{fly}} = \sum_{n=1}^{N} P_0\left(\left(1+\frac{3\|\boldsymbol{v}_k[n]\|^2}{U_{\text{tip}}^2}\right)+\frac{P_i V_0}{\lambda_{k,n}} + \frac{1}{2}d_0\epsilon s M\|\boldsymbol{v}_k[n]\|^3\right)\delta_t \tag{18}$$

with additional constraint

$$\|\boldsymbol{v}_k[n]\|^2 \ge \lambda_{k,n}^2 \tag{19}$$

$$\lambda_{k,n} \ge 0 \tag{20}$$

In terms of the coupled variables $\boldsymbol{v}_k[n]$ and $\lambda_{k,n}$, it can be easily confirmed that the (18) exists a convex structure. However, a new nonconvex constraint is introduced to the relaxed constraint of (19). To handle it, the SCA technique is applied [36]. More precisely, under a given local point $\{\boldsymbol{v}_{k,l}[n]\}$ over l-th iteration, we obtain

$$\begin{aligned}\|\boldsymbol{v}_k[n]\|^2 &\geq \|\boldsymbol{v}_{k,l}[n]\|^2 + 2\boldsymbol{v}_{k,l}^{\mathrm{T}}[n](\boldsymbol{v}_k[n]-\boldsymbol{v}_{k,l}[n])\\ &= f^{\mathrm{lb}}(\boldsymbol{v}_k[n])\end{aligned} \tag{21}$$

Formula (21) accords with the fact of the global under-estimator can be obtained by applying the first-order Taylor expansion to the convex function [37]. What is noteworthy is that $f^{\mathrm{lb}}(\boldsymbol{v}_k[n])$ is a linear function in regard to $\boldsymbol{v}_k[n]$. Consequently, the constraint (19) can be rewritten as

$$f^{lb}(\boldsymbol{v}_k[n]) \geq \lambda_{k,n}^2 \tag{22}$$

In the following, we tackle the nonconvex constraint (8). Similarly, at a given point $\{\boldsymbol{u}_{k,l}[n]\}$ and $\{\boldsymbol{u}_{j,l}[n]\}$ to $\|\boldsymbol{u}_k[n]-\boldsymbol{u}_j[n]\|^2$, we apply the first-order Taylor expansion. Therefore, we can get

$$\begin{aligned}&\|\boldsymbol{u}_k[n]-\boldsymbol{u}_j[n]\|^2\\ &\geq -\|\boldsymbol{u}_k[n]-\boldsymbol{u}_j[n]\|^2\\ &\quad + 2(\|\boldsymbol{u}_{k,l}[n]-\boldsymbol{u}_{j,l}[n]\|^2)^{\mathrm{T}}(\boldsymbol{u}_{k,l}[n]-\boldsymbol{u}_{j,l}[n])\\ &= \boldsymbol{S}_{k,j}^{\mathrm{lb}}[n]\end{aligned} \tag{23}$$

Subsequently, we introduce slack variable $\{\boldsymbol{y}_{k,m}[n]\}$ to relax constraint (14d) in order to address the nonconvex constraint (14d), then the constraint (14d) is reformulated as

$$\begin{aligned}&\sum_{n=1}^{N}\sum_{m=1}^{M}\left(\alpha_{k,m}[n]B\log_2\left(1+\frac{\phi}{\boldsymbol{y}_{k,m}[n]+H}\right)\right)\delta_t\\ &\quad\geq (1-\rho_k)L_k\end{aligned} \tag{24}$$

and

$$\|\boldsymbol{u}_k[n]-\boldsymbol{w}_m\|^2 \leq \boldsymbol{y}_{k,m}[n] \tag{25}$$

where $\phi = p_k[n]\beta_0/\sigma^2$ denotes the product of the transmitting power of UAV k and reference signal-to-noise (SNR), $H=(H_2-H_1)^2$ represents the square of the height difference between UAVs and HABs. In the same way, over l-th iteration, under the given local point $\left\{\boldsymbol{y}_{k,m}^{l}[n]\right\}$, we take the first-order Taylor expansion of the left hand side in constraint (24), the following global lower bound is calculated as

$$\begin{aligned}\alpha_{k,m}[n]B\log_2\left(1+\frac{\phi}{\boldsymbol{y}_{k,m}[n]+H}\right) &\geq \boldsymbol{B}_{k,m}[n]-\boldsymbol{C}_{k,m}[n]\\ &= \boldsymbol{R}_{k,m}^{\mathrm{lb}}[n]\end{aligned} \tag{26}$$

where

$$\boldsymbol{B}_{k,m}[n] = \frac{\alpha_{k,m}[n]B}{\ln 2}[\ln(\boldsymbol{y}_{k,m}^{l}[n]+H+\phi)-\ln(\boldsymbol{y}_{k,m}^{l}[n]+H)]$$

and

$$\begin{aligned}\boldsymbol{C}_{k,m}[n] = &\frac{\alpha_{k,m}[n]B\phi}{\ln 2(\boldsymbol{y}_{k,m}^{l}[n]+H+\phi)(\boldsymbol{y}_{k,m}^{l}[n]+H)}\\ &\times(\boldsymbol{y}_{k,m}[n]-\boldsymbol{y}_{k,m}^{l}[n])\end{aligned}$$

By leveraging the lower bound on a given local point obtained above, we make the corresponding substitution of the nonconvex objective function and nonconvex constraints (8), (14d) in (P2.2), then the optimization problem after transformation is shown as

$$\text{P2.3:}\quad \min_{\boldsymbol{U},\{\lambda_{k,n}\}\{y_{k,m}[n]\}} \sum_{k=1}^{K}E_k^{\mathrm{loc}}+\sum_{k=1}^{K}E_k^{\mathrm{comm}}+\sum_{k=1}^{K}\overline{E}_k^{\mathrm{fly}} \tag{27a}$$

$$\text{s.t.}\quad \boldsymbol{S}_{k,j}^{\mathrm{lb}}[n] \geq d_{\min}^2 \tag{27b}$$

$$\sum_{n=1}^{N}\sum_{m=1}^{M}\boldsymbol{R}_{k,m}^{\mathrm{lb}}[n]\delta_t \geq (1-\rho_k)L_k \tag{27c}$$

$$\text{Eqs. (5), (6), (7), (20), (22), (25)} \tag{27d}$$

It can be shown that the problem (P2.3) has a convex structure and can be settled efficiently using standard convex techniques.

3. Joint algorithm design

In view of the results of the previous two parts, we put forward an overall iterative algorithm by making use of the BCD method in terms of the original problem (P1). In particular, the entire optimization variable is divided into two blocks, i.e., $\{\boldsymbol{A},\boldsymbol{\varrho}\}$ and $\boldsymbol{U}$. Subsequently, the UAV-HAB association $\boldsymbol{A}$, the calculation task splitting ratio $\boldsymbol{\varrho}$, and the UAV trajectory $\boldsymbol{U}$ are alternately optimized by settling problem (P2.1) and (P2.3) correspondingly. In addition, the input of the next iteration is the obtained solution in each iteration. The process continues until the value of the objective function converges, as dipicted in Figure 2. The specifics of this algorithm are outlined in Algorithm 1.

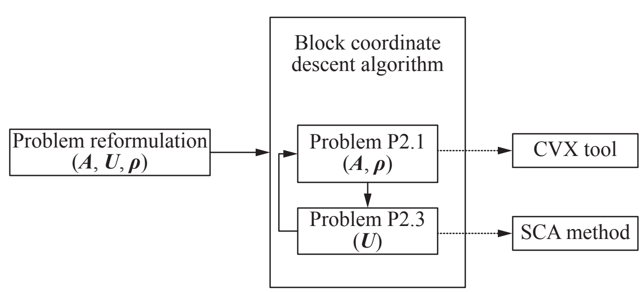

Figure 2 The procedure of Algorithm 1.

Algorithm 1 Block coordinate descent algorithm for problem P2

Initialize $\left\{\boldsymbol{U}^0, \lambda_{k,n}^0, y_{k,m}^0[n]\right\}$, $r=0$;
repeat

3: Solve problem P2.1 under the given $\{\boldsymbol{U}^r\}$, and denote the optimal solution as $\{\boldsymbol{A}^{r+1}, \boldsymbol{\varrho}^{r+1}\}$;

4: Solve problem P2.3 under the given $\{\boldsymbol{A}^{r+1}, \boldsymbol{\varrho}^{r+1}, \lambda_{k,n}^{r}, y_{k,m}^{r}[n]\}$, and denote the optimal solution as $\left\{\boldsymbol{U}^{r+1}, \lambda_{k,n}^{r+1}, y_{k,m}^{r+1}[n]\right\}$;

5: $r = r + 1$;

6: **until** the incremental growth of the target value falls below a specified threshold $\varsigma > 0$

V. Complexity and Convergence Analysis

In this section, we first concisely analyze the computational complexity of Algorithm 1.

- Complexity analysis: To solve the UAV-HAB association of problem (16), the complexity of updating the UAV-HAB association is $\mathcal{O}(NKM)$, and the complexity to solve the problem (P2.3) is $\mathcal{O}(N(K(K-1)+KM))$, in addition, the count of external iterations is E. Then the overall complexity of Algorithm 1 can be obtained as follows:

$$\mathcal{O}[E(NKM + N(K(K-1) + KM))] \tag{28}$$

- Convergence analysis: We then analyze the convergence of Algorithm 1. It is noted that in the classical BCD algorithm, the subproblem of updating each variable block needs to be settled precisely with optimality in each iteration to ensure the final convergence. But in the issue we solved, the trajectory optimization problem (P2.2), we can solely achieve an optimal solution for its approximate problem (P2.3). Therefore, it is necessary to prove the convergence of Algorithm 1, instead of directly applying the related convergence analysis of classical BCD algorithm.

We denote the objective value of the original problem (P2) as $\Phi(\boldsymbol{A}, \boldsymbol{U}, \boldsymbol{\varrho})$. In the third step of Algorithm 1, since $\{\boldsymbol{A}^{r+1}, \boldsymbol{\varrho}^{r+1}\}$ is one subopimal UAV-HAB association and calculation task splitting ratio of problem (P2.1) with the fixed $\{\boldsymbol{U}^r\}$, we have

$$\Phi(\boldsymbol{A}^r, \boldsymbol{U}^r, \boldsymbol{\varrho}^r) \geq \Phi(\boldsymbol{A}^{r+1}, \boldsymbol{U}^r, \boldsymbol{\varrho}^{r+1}) \tag{29}$$

In step 4 of Algorithm 1, for given $\{\boldsymbol{A}^{r+1}, \boldsymbol{\varrho}^{r+1}\}$, $\{\boldsymbol{U}^r\}$ is one subopimal UAV trajectory of problem (P2.3), it follows that

$$\Phi(\boldsymbol{A}^{r+1}, \boldsymbol{U}^r, \boldsymbol{\varrho}^{r+1}) \geq \Phi(\boldsymbol{A}^{r+1}, \boldsymbol{U}^{r+1}, \boldsymbol{\varrho}^{r+1}) \tag{30}$$

From the analysis presented above, we can conclude

$$\Phi(\boldsymbol{A}^r, \boldsymbol{U}^r, \boldsymbol{\varrho}^r) \geq \Phi(\boldsymbol{A}^{r+1}, \boldsymbol{U}^{r+1}, \boldsymbol{\varrho}^{r+1}) \tag{31}$$

Formula (31) shows that the target value of problem (P2) does not increase after each iteration of Algorithm 1. Given that the objective value of problem (P2) serves as the lower bound of a finite value, the convergence of the proposed Algorithm 1 is guaranteed. In Section V, the numerical results show that the proposed BCD method converges rapidly for the settings we consider. Additionally, in per iteration of Algorithm 1, it only needs to solve complex convex optimization problems of polynomials, the algorithm proposed in this paper can actually achieve a network with a medium number of cellular-connected multi-UAV with fast convergence.

VI. Numerical Results

This section demonstrate the effectiveness of our proposed algorithm through numerical results. The height of UAVs and three HABs are fixed at $H_1 = 500$ m and $H_2 = 2500$ m, respectively. Based on the previous statement in Section III, $\Delta H_2 \in [-1, 1]$. The transmission power of UAVs during any time slot n and the maximum speed of UAVs are set as $p_k[n] = 2$ W and $\boldsymbol{v}_{\max} = 30$ m/s, respectively. Some other parameters are listed in Table 1.

Table 1 Parameter value setting

Ω	400 radians/s	N	1000
r	0.5 m	β_0	−30 dB
U_{tip}	Ωr	σ^2	−60 dBm
ϵ	1.225 kg/m^3	B	50 MHz
M	0.79 m^2	C_{u}	500 cycle/bit
P_{i}	79.07 W	D_{u}	2 GHz
V_0	3.6 m/s	d_0	0.075
d_0	0.075	s	0.01
λ	100	ς	10^{-3}
P_0	29.03 W	P_{u}	9.5×10^{-11} J/Cycle

It is imperative to first ensure the convergence of the proposed iterative algorithm during execution. Figure 3 and Figure 4 show the trend of the total energy consumption of all UAVs with respect to the number of iterations under different task quantity L and time period T, respectively. In particular, Figure 3 depicts the total energy consumption of all UAVs of the proposed iterative algorithm for different task quantity L versus the number of iterations. It can be seen from Figure 3 that the larger the task quantity L is, the higher the total en-

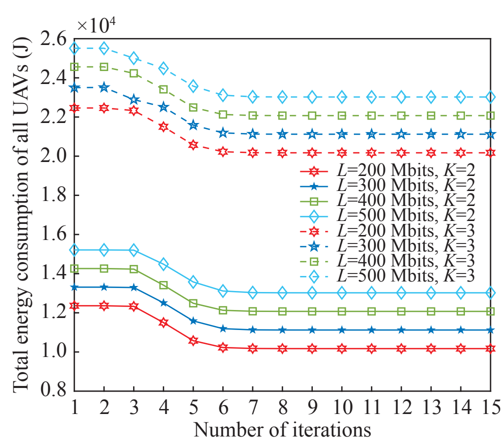

Figure 3 Comparison on the proposed algorithm convergence with different task quantity L for time period $T = 100$ s.

ergy consumption of all UAVs is. Meanwhile, it is not difficult to see that the cumulative energy consumption of all UAVs is increased as K increases. Specifically, Figure 4 shows the total energy consumption of all UAVs of the proposed iterative algorithm for different time period T versus the number of iterations. It can be observed from Figure 4 that the longer the time period T is, the higher the total energy consumption of all UAVs is. Additionally, it is worth noting that in Figure 3 and Figure 4, after only eight iterations, the proposed iterative algorithm achieves convergence for all considered cases. Besides, the convergence speed of the proposed algorithm is invariant to different task quantity L or different time period T, which is expected for practical system deployment.

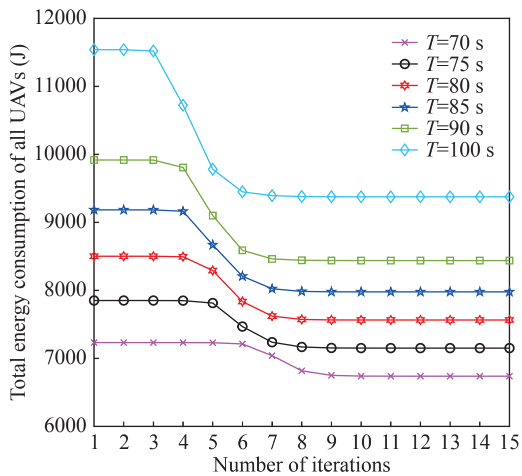

Figure 4 Comparison on the proposed algorithm convergence with different task period T for task quantity L = 100 Mbits and K = 2.

The optimized two UAVs' trajectories with time period T = 100 s are depicted in Figure 5. The initial position and final position of UAV 1 are set as $\boldsymbol{u}_{1,\mathrm{I}} = [-500, -500]^{\mathrm{T}}$ and $\boldsymbol{u}_{1,\mathrm{F}} = [500, -500]^{\mathrm{T}}$, respectively, and the initial position and end position of UAV 2 are respectively set as $\boldsymbol{u}_{2,\mathrm{I}} = [-500, 500]^{\mathrm{T}}$ and $\boldsymbol{u}_{2,\mathrm{F}} = [500, 500]^{\mathrm{T}}$. Their initial velocity are both set as $\boldsymbol{v}_{\mathrm{k}}[0] = [10, 10]^{\mathrm{T}}$, $k \in \{1, 2\}$. Additionally, the horizontal coordinates of the three HABs are set as $\boldsymbol{w}_1 = [-300, 0]^{\mathrm{T}}$, $\boldsymbol{w}_2 = [0, 0]^{\mathrm{T}}$, and

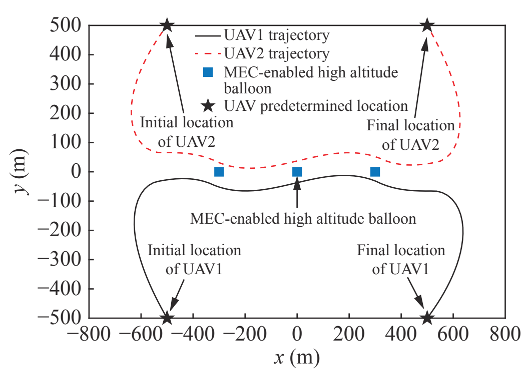

Figure 5 UAVs' trajectories with TDMA scheme for T = 100 s.

$\boldsymbol{w}_3 = [300, 0]^{\mathrm{T}}$. There are two things we can observe in Figure 5. Intuitively, the UAVs' trajectories curve will mostly produce straight flight, which denotes that the energy minimization strategy is a simple straight-line method when the UAV's speed remains unchanged. Another observation is that UAVs prefer to reposition themselves to move close to HABs, which means that the more bits will be migrated to HABs for computation and less energy will be consumed by the UAVs for local computation.

Moreover, we apply the following two benchmark designs to verify the effectiveness of the proposed scheme:

Straight Flight In this case, the UAV flies along a straight trajectory.

Local Computation Under this circumstance, tasks are limited to local processing on each individual UAV.

Figure 6 demonstrates the overall energy cost versus the mission period T for mission quantity L = 100 Mbits. According to Figure 6, as the time period T increases, the energy consumed by the local computation increases rapidly. Compared with the local calculation design, the other designs achieve smaller energy consumption values. It can be explained by the fact that HAB as a helper can assist task computing. Moreover, we can see that the proposed design exceeds the other designs because of the optimization of UAV-HAB association and calculation task splitting ratio as well as UAV trajectory.

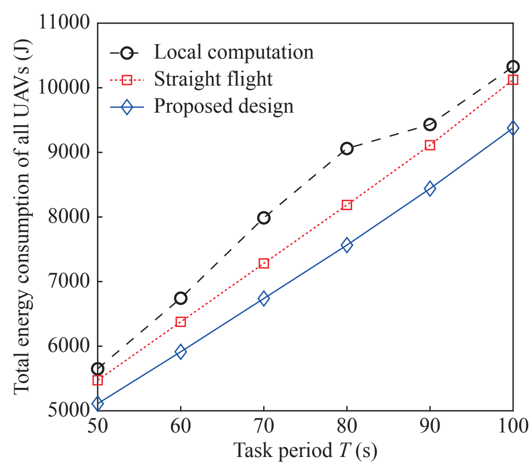

Figure 6 Total energy consumption of all UAVs vs. task period T (L = 100 Mbits).

Figure 7 depicts the total energy consumption with the proposed design and the benchmark scheme over different mission quantity under different number of HABs M. We noticed that the designs we come up with always exhibits better performance than other designs, and this advantage become more and more obvious as the mission volume of each UAV increased. This is expected in our proposed design, UAVs can optimize their trajectories to achieve significant reductions in local computing energy consumption, communication energy consumption, and flight energy consumption. Furthermore, because of the fixed trajectory pattern, the straight-line flight design is limited in maneuverability development relative to the proposed design and consumes more energy. Meanwhile, it is also observed that the overall energy consumption of all UAVs diminishes with the growth of M, which is expected since the increasing number of HABs inevitably enhanced communication performance between the UAV and nearby HABs.

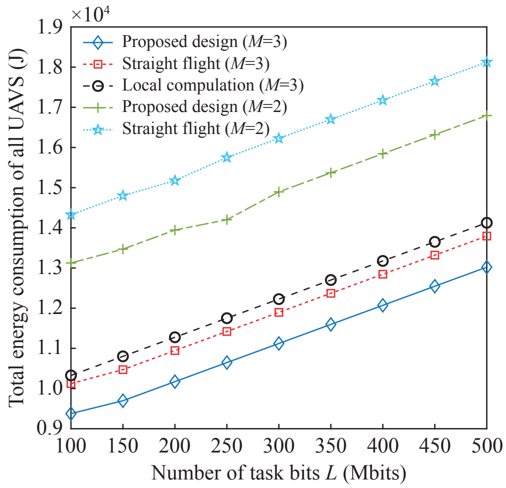

Figure 7 Total energy consumption of all UAVs vs. task quantity L ($T = 100$ s).

In Figure 8, a simple comparison between the flight energy cost and the local calculation energy cost is made. As expected, the task period T has a significant effect on local calculation energy consumption. With the increase of T, the local calculation of energy consumption of UAVs almost approaches zero. This can be explained that UAVs have more time to offload tasks to HABs and then reduce their calculation energy consumption. Moreover, we can easily notice that the flight energy cost of UAVs nondecreases as the task period T increases. There is no doubt that the longer a UAV flies, the more energy it will consume.

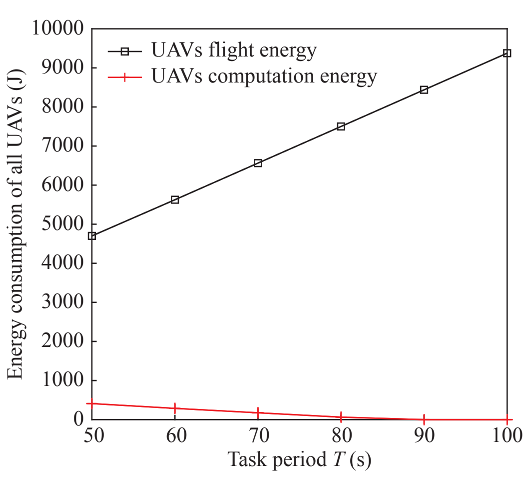

Figure 8 A comparison between UAV's flight energy consumption and calculate energy consumption with different T (L = 100 Mbits).

VII. Conclusions

In this paper, we proposed a new MEC application scene where multi-UAV offload their calculation tasks to multi-HAB during their flight. The UAVs' trajectories were jointly designed with the computation task splitting to minimize the total energy cost of all UAVs, subject to the mission maximum processing delays, UAV's maximum speed, and initial/termination position restrictions. By using SCA technology and an alternating iterative approach, an effective algorithm for solving the formulated problem was proposed. Numerical results were conducted to show that our proposed design can reduce the UAV energy consumption by 10% and 20% compared with the Straight Flight design and Local Computation design, respectively. In future work, we will further take into account the influence of the heights of UAVs and HABs on the energy consumption of all UAVs.

Acknowledgements

This work was supported by the National Key Research and Development Program of China (Grant No. 2021ZD0112200).

References

[1] D. Wang, J. Tian, H. X. Zhang, *et al.*, "Task offloading and trajectory scheduling for UAV-enabled MEC networks: An optimal transport theory perspective," *IEEE Wireless Communications Letters*, vol. 11, no. 1, pp. 150–154, 2022.

[2] J. N. Chen, S. Y. Chen, S. Y. Luo, *et al.*, "An intelligent task offloading algorithm (iTOA) for UAV edge computing network," *Digital Communications and Networks*, vol. 6, no. 4, pp. 433–443, 2020.

[3] G. Y. Wu and J. C. Gu, "Remote interference source localization: A multi-UAV-based cooperative framework," *Chinese Journal of Electronics*, vol. 31, no. 3, pp. 442–455, 2022.

[4] B. Li, Z. S. Fei, and Y. Zhang, "UAV communications for 5G and beyond: Recent advances and future trends," *IEEE Internet of Things Journal*, vol. 6, no. 2, pp. 2241–2263, 2019.

[5] L. Yang, H. P. Yao, J. J. Wang, *et al.*, "Multi-UAV-enabled load-balance mobile-edge computing for IoT networks," *IEEE Internet of Things Journal*, vol. 7, no. 8, pp. 6898–6908, 2020.

[6] H. D. Li, F. Fang, and Z. G. Ding, "Joint resource allocation for hybrid NOMA-assisted MEC in 6G networks," *Digital Communications and Networks*, vol. 6, no. 3, pp. 241–252, 2020.

[7] M. Wang, S. Shi, S. S. Gu, *et al.*, "*Q*-learning based computation offloading for multi-UAV-enabled cloud-edge computing networks," *IET Communications*, vol. 14, no. 15, pp. 2481–2490, 2020.

[8] X. H. Gu, G. A. Zhang, M. X. Wang, *et al.*, "UAV-aided energy-efficient edge computing networks: Security offloading optimization," *IEEE Internet of Things Journal*, vol. 9, no. 6, pp. 4245–4258, 2022.

[9] L. Sun, L. T. Wan, and X. P. Wang, "Learning-based resource allocation strategy for industrial IoT in UAV-enabled MEC systems," *IEEE Transactions on Industrial Informatics*, vol. 17, no. 7, pp. 5031–5040, 2021.

[10] B. Y. Liu, Y. Y. Wan, F. H. Zhou, *et al.*, "Resource allocation and trajectory design for MISO UAV-assisted MEC networks," *IEEE Transactions on Vehicular Technology*, vol. 71, no. 5, pp. 4933–4948, 2022.

[11] G. S. Yang, L. Hou, X. Y. He, *et al.*, "Offloading time optimization via Markov decision process in mobile-edge computingd," *IEEE Internet of Things Journal*, vol. 8, no. 4, pp. 2483–2493, 2021.

[12] B. D. Shang and L. J. Liu, "Mobile-edge computing in the

sky: Energy optimization for air-ground integrated networks," *IEEE Internet of Things Journal*, vol. 7, no. 8, pp. 7443–7456, 2020.
[13] X. F. Chen, C. Wu, Z. Liu, *et al.*, "Computation offloading in beyond 5G networks: A distributed learning framework and applications," *IEEE Wireless Communications*, vol. 28, no. 2, pp. 56–62, 2021.
[14] Y. Q. Li, X. Wang, X. Y. Gan, *et al.*, "Learning-aided computation offloading for trusted collaborative mobile edge computing," *IEEE Transactions on Mobile Computing*, vol. 19, no. 12, pp. 2833–2849, 2020.
[15] L. Xiao, X. Z. Lu, T. W. Xu, *et al.*, "Reinforcement learning-based mobile offloading for edge computing against jamming and interference," *IEEE Transactions on Communications*, vol. 68, no. 10, pp. 6114–6126, 2020.
[16] J. F. Liu, L. X. Li, F. C. Yang, *et al.*, "Minimization of offloading delay for two-tier UAV with mobile edge computing," in *Proceedings of the 15th International Wireless Communications & Mobile Computing Conference*, Tangier, Morocco, pp.1534–1538, 2019.
[17] X. B. Cao, P. Yang, M. Alzenad, *et al.*, "Airborne communication networks: A survey," *IEEE Journal on Selected Areas in Communications*, vol. 36, no. 9, pp. 1907–1926, 2018.
[18] Z. Z. Xu, C. L. Chen, Y. Guo, *et al.*, "Ballooning: An agent-based search strategy in wireless sensor and actor networks," *IEEE Communications Letters*, vol. 15, no. 9, pp. 944–946, 2011.
[19] M. Mozaffari, W. Saad, M. Bennis, *et al.*, "A tutorial on UAVs for wireless networks: Applications, challenges, and open problems," *IEEE Communications Surveys & Tutorials*, vol. 21, no. 3, pp. 2334–2360, 2019.
[20] Y. M. Liu, D. Grace, and P. D. Mitchell, "Exploiting platform diversity for GoS improvement for users with different high altitude platform availability," *IEEE Transactions on Wireless Communications*, vol. 8, no. 1, pp. 196–203, 2009.
[21] A. Ibrahim and A. S. Alfa, "Using lagrangian relaxation for radio resource allocation in high altitude platforms," *IEEE Transactions on Wireless Communications*, vol. 14, no. 10, pp. 5823–5835, 2015.
[22] C. Zhan, H. Hu, Z. Liu, *et al.*, "Multi-UAV-enabled mobile-edge computing for time-constrained IoT applications," *IEEE Internet of Things Journal*, vol. 8, no. 20, pp. 15553–15567, 2021.
[23] Y. Liu, S. L. Xie, and Y. Zhang, "Cooperative offloading and resource management for UAV-enabled mobile edge computing in power IoT system," *IEEE Transactions on Vehicular Technology*, vol. 69, no. 10, pp. 12229–12239, 2020.
[24] Z. Y. Yang, S. Z. Bi, and Y. J. A. Zhang, "Dynamic trajectory and offloading control of UAV-enabled MEC under user mobility," in *Proceedings of IEEE International Conference on Communications Workshops*, Montreal, QC, Canada, pp.1–6, 2021.
[25] X. W. Cao, J. Xu, and R. Zhang, "Mobile edge computing for cellular-connected UAV: Computation offloading and trajectory optimization," in *Proceedings of the 19th International Workshop on Signal Processing Advances in Wireless Communications*, Kalamata, Greece, pp.1–5, 2018.
[26] A. A. A. Ateya, A. Muthanna, R. Kirichek, *et al.*, "Energy-and latency-aware hybrid offloading algorithm for UAVs," *IEEE Access*, vol. 7, pp. 37587–37600, 2019.
[27] M. Hua, Y. M. Huang, Y. Sun, *et al.*, "Energy optimization for cellular-connected UAV mobile edge computing systems," in *Proceedings of IEEE International Conference on Communication System*, Chengdu, China, pp.1–6, 2018.
[28] Z. H. Lv, J. J. Hao, and Y. J. Guo, "Energy minimization for MEC-enabled cellular-connected UAV: Trajectory optimization and resource scheduling," in *Proceedings of IEEE Conference on Computer Communications Workshops*, Toronto, ON, Canada, pp.478–483, 2020.
[29] M. Hua, Y. M. Huang, Y. Wang, *et al.*, "Energy optimization for cellular-connected multi-UAV mobile edge computing systems with multi-access schemes," *Journal of Communications and Information Networks*, vol. 3, no. 4, pp. 33–44, 2018.
[30] C. W. Wang, Y. L. Cui, D. H. Deng, *et al.*, "Trajectory optimization and power allocation scheme based on DRL in energy efficient UAV-aided communication networks," *Chinese Journal of Electronics*, vol. 31, no. 3, pp. 397–407, 2022.
[31] Y. W. Huang, J. Xu, L. Qiu, *et al.*, "Cognitive UAV communication via joint trajectory and power control," in *Proceedings of IEEE 19th International Workshop on Signal Processing Advances in Wireless Communications*, Kalamata, Greece, pp.1–5, 2018.
[32] N. N. Ei, S. W. Kang, M. Alsenwi, *et al.*, "Multi-UAV-assisted MEC system: Joint association and resource management framework," in *Proceedings of the International Conference on Information Networking*, Jeju Island, Korea (South), pp.213–218, 2021.
[33] Y. Xu, T. K. Zhang, D. C. Yang, *et al.*, "Joint resource and trajectory optimization for security in UAV-assisted MEC systems," *IEEE Transactions on Communications*, vol. 69, no. 1, pp. 573–588, 2021.
[34] T. Bai, J. J. Wang, Y. Ren, *et al.*, "Energy-efficient computation offloading for secure UAV-edge-computing systems," *IEEE Transactions on Vehicular Technology*, vol. 68, no. 6, pp. 6074–6087, 2019.
[35] Y. Zeng, J. Xu, and R. Zhang, "Energy minimization for wireless communication with rotary-wing UAV," *IEEE Transactions on Wireless Communications*, vol. 18, no. 4, pp. 2329–2345, 2019.
[36] S. Yue, J. Ren, N. Qiao, *et al.*, "TODG: Distributed task offloading with delay guarantees for edge computing," *IEEE Transactions on Parallel and Distributed Systems*, vol. 33, no. 7, pp. 1650–1665, 2022.
[37] D. W. Matolak and R. Y. Sun, "Air-ground channel characterization for unmanned aircraft systems-part Ⅲ: The suburban and near-urban environments," *IEEE Transactions on Vehicular Technology*, vol. 66, no. 8, pp. 6607–6618, 2017.

Jingming XIA was born in Jiangsu Province in 1980. He received the B.S. and M.S. degrees in information engineering and the Ph.D. degree in atmospheric science from the Nanjing University of Information Science and Technology, Nanjing, China, in 2005 and 2012, respectively. He is currently an Professor with the Artificial Intelligence Department, Nanjing University of Information Science and Technology. He is the author of two books and more than 30 articles. His research interests include the application of machine learning and deep learning in meteorology.
(Email: xiajingming@nuist.edu.cn)

Yufeng LIU was born in Hebei Province in 1996. She received the B.S. degree in information engineering from Hebei GEO University, Shijiazhuang, China, in 2020. Since 2020, she has been working towards the M.S. degree in the School of Computer and Software, Nanjing University of Information Science and Technology. Her current research interests include unmanned-aerial-vehicle communications, mobile-edge computing, and machine learning.
(Email: yufengliu@nuist.edu.cn)

Ling TAN was born in Jiangsu Province in 1979. She received the B.S. and M.S. degrees in information engineering from Nanjing Normal University, in 2005, and the Ph.D. degree in information and network from the Nanjing University of Posts and Telecommunications, Nanjing, in 2012. Since 2020, she has been an Professor with the School of Computer and Software, Nanjing University of Information Science and Technology. She is the author of 3 books and more than 20 articles. Her research interests include the application of machine learning and deep learning in image processing.
(Email: cillatan0@nuist.edu.cn)